

## THE STUDY OF TOROIDAL REGENERATIVE TURBOMACHINE USING THE FINITE VOLUME METHOD AND SOLA ALGORITHM

**Marcelo José Pirani**

Federal University of Itajubá - UNIFEI, Ave. BPS, 1303, Pinheirinho, Itajubá, MG, Brasil, CEP: 37500-903.  
e-mail: pirani@iem.efei.br

**Nelson Manzanares Filho**

Federal University of Itajubá - UNIFEI, Ave. BPS, 1303, Pinheirinho, Itajubá, MG, Brasil, CEP: 37500-903.  
e-mail: nelson@iem.efei.br

**Manuel da Silva Valente de Almeida**

Federal University of Itajubá - UNIFEI, Ave. BPS, 1303, Pinheirinho, Itajubá, MG, Brasil, CEP: 37500-903.

**Abstract.** With the finite volume method and SOLA algorithm, a study of turbulent two-dimensional flow in a toroidal regenerative turbomachine is carried out. The equations representing the fluid flow in cartesian coordinates are transformed into a coordinate system specially developed for this machine. The two-equation turbulence model  $\kappa$ - $\epsilon$  and the convective scheme "QUICK" are employed. The resulting equation system is solved by Choleski method. Results for the slip factor, head coefficient, and vorticity are presented and compared with literature.

**Keywords.** Toroidal Regenerative Turbomachine, Side Channel Regenerative Turbomachine, Finite Volumes, SOLA Algorithm,  $\kappa$ - $\epsilon$  Turbulence Model.

### 1. Introduction

The regenerative turbomachine is a special kind of fluid machine normally used as a pump, compressor or blower. The scheme of a toroidal (or side channel) regenerative turbomachine is shown in Figure (1). It is particularly suitable where high pressure and low flow rate are required. Its simplicity of construction and stable operating characteristics have made this kind of machine more attractive to use in several applications, including textile, graph and nutritious industries, agriculture, medicine, products transport, and others. They presents efficiency relatively low, however, when compared to the centrifugal pumps, that need several stages to reach the same pressure level, its efficiency can be compared.

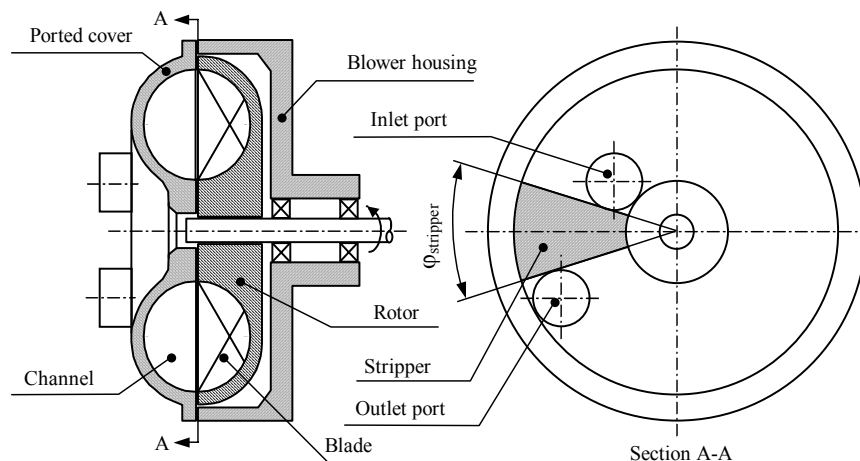


Figure 1. Toroidal regenerative turbomachine.

Several working processes and consequent theories, concerning the description of the internal flow in regenerative turbomachines, have been proposed, but there are essentially two main types, namely, the Turbulence and the Circulatory theory. This classification corresponds to the adopted hypotheses concerning the mechanism of momentum transfer from the impeller to the working fluid in the channel. The working principle adopted in this work is the same of the Circulatory theory. According to this principle, the working fluid flows in a helical path along the impeller and annular channel from the inlet to outlet port. The circulatory flow is created from the action of centrifugal forces in the fluid particles on the impeller blade region. The fluid gains angular momentum when passes between the rotor blades and loses the angular momentum when goes by the lateral channel, creating a pressure increase. This process occurs several times along the machine, maintaining a pressure gradient in the circumferential direction.

The toroidal regenerative turbomachine and some characteristic dimensions are presented in Figure 2.

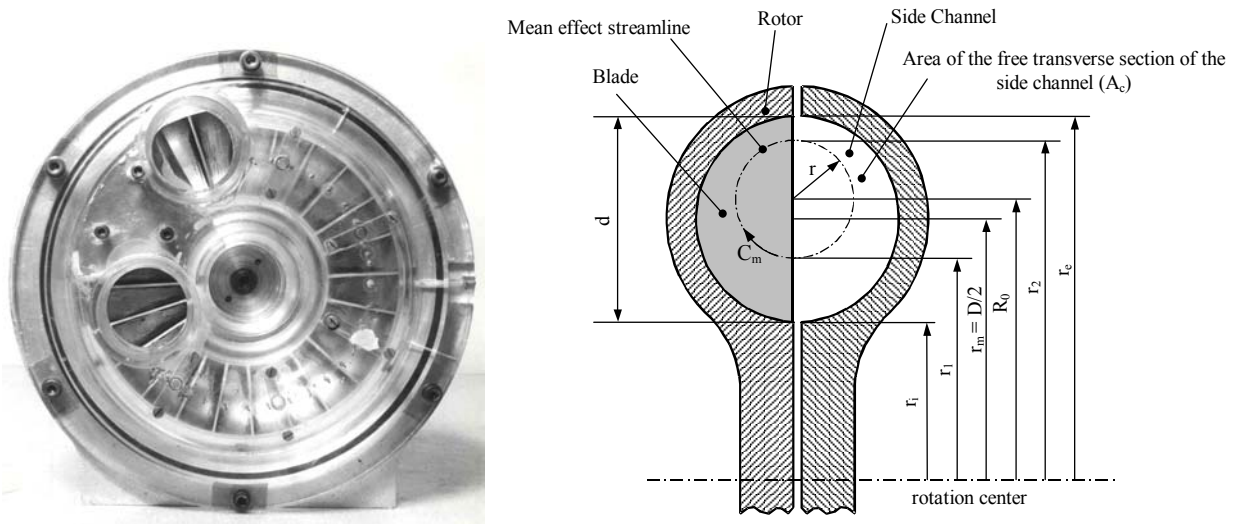


Figure 2. Toroidal regenerative turbomachine and scheme with characteristic dimensions of the blade and side channel.

## 2. Flow Region

For a better understanding of the development presented in the subsequent items of the present work, it is important to define the flow region inside of the toroidal regenerative turbomachine. In Figure 3, a simplified scheme of a toroidal regenerative turbomachine is shown, on which the region of the flow is enlarged to clarify. For a fixed value of the radius,  $r$ , the flow surface is limited between two consecutive blades, by the surfaces that go parallel to these blades. Cutting the flow surface along the line  $a-a'$  and representing it on a plan, it is possible to obtain the region shown in Figure 4. This is the region on which the whole modelling of the toroidal regenerative turbomachine is developed. The effectiveness of the one-dimensional analytic treatment of the toroidal regenerative turbomachine depends on the correct determination of the so called “mean effect streamline” of the flow. This line is the main connection element between the hydrodynamic and geometric parameters of the machine. The equations in the present work are of use if the flow surface is defined by the representative radius of the mean effect streamline, which is obtained from the experimental data of Varella (1981).

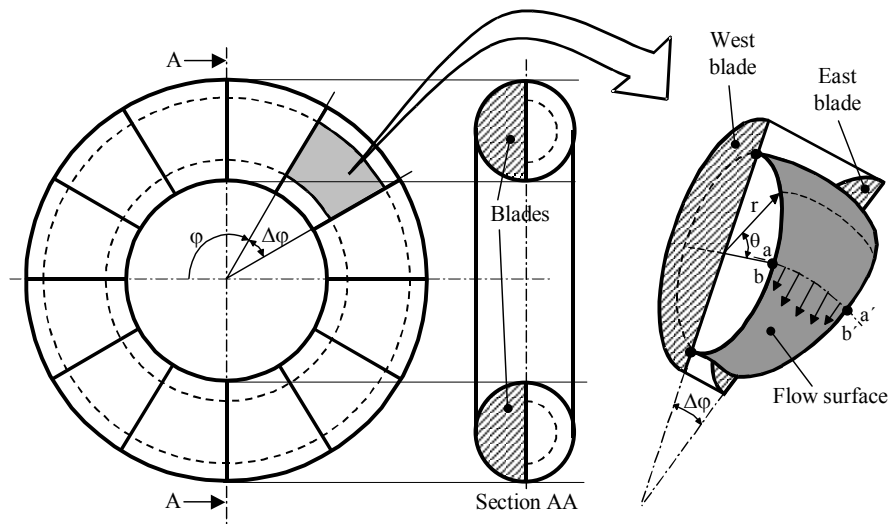


Figure 3. Simplified scheme of the toroidal regenerative turbomachine and detail of the flow region enlarged.

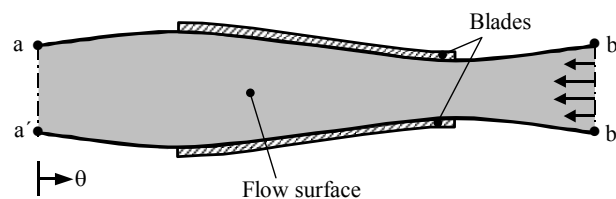


Figure 4. Flow region represented in an idealized plane surface.

### 3. Coordinate transformation and governing equations

#### 3.1. Coordinate transformation

To model the flow in the toroidal regenerative turbomachine, a coordinate transformation is made starting from the Cartesian coordinates. The representative equations of the flow are obtained in the new coordinate system. Figure 5 shows the coordinate system proposed for the toroidal regenerative turbomachine in Figure 1.

Flow equations in the proposed coordinate system  $(r, \varphi, \theta)$  is developed through the following steps:

- Write the equation in tensor invariant form;
- Development of the metric coefficients corresponding to the proposed transformation relationships;
- Obtain from the literature, the formulae for the Gradient, Divergence, Laplacian and Curl operators in general orthogonal curvilinear coordinates;
- In these formulae, substitute the metric coefficients, as well, the velocity components  $V_r$ ,  $V_\varphi$  and  $V_\theta$ , in order to obtain particular operator formulae in the coordinates of the toroidal regenerative turbomachine;
- With the operators written in the proposed toroidal coordinates, the representative equations of the flow in the regenerative turbomachine are finally obtained.

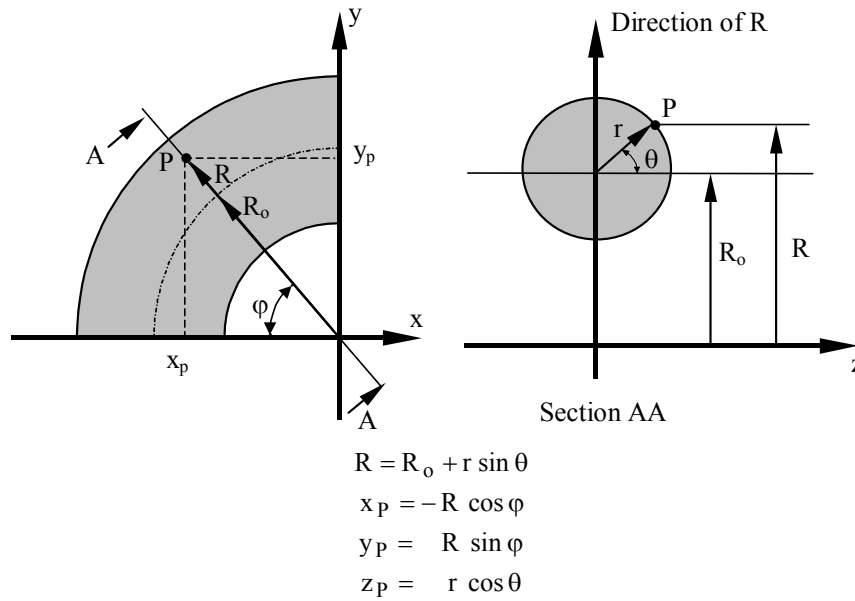


Figure 5. Toroidal regenerative turbomachine coordinates and transformation relationships.

#### 3.2. Governing equations

The continuity and momentum equations in the toroidal regenerative turbomachine coordinates, after have been accomplished by the Reynolds decomposition and considered the rotation effects, take the form:

- Average continuity equation

$$\frac{1}{R} \frac{\partial V_\varphi}{\partial \varphi} + \frac{1}{r} \frac{\partial V_\theta}{\partial \theta} + \frac{V_\theta \cos \theta}{R} = 0 \quad (1)$$

- Average momentum equation in  $\varphi$  and  $\theta$  direction, respectively.

$$\begin{aligned} \frac{\partial V_\varphi}{\partial t} + \frac{1}{R} \frac{\partial}{\partial \varphi} \left[ V_\varphi V_\varphi - \frac{\nu}{R} \frac{\partial V_\varphi}{\partial \varphi} + \overline{v'_\varphi v'_\varphi} \right] + \frac{1}{Rr} \frac{\partial}{\partial \theta} \left[ R V_\varphi V_\theta - \frac{\nu R}{r} \frac{\partial V_\varphi}{\partial \theta} + R \overline{v'_\varphi v'_\theta} \right] = \\ - \frac{1}{\rho R} \frac{\partial P}{\partial \varphi} - \frac{V_\varphi V_\theta}{R} \cos \theta - \frac{\overline{v'_\varphi v'_\theta}}{R} \cos \theta + \nu \left[ \frac{2 \cos \theta}{R^2} \frac{\partial V_\theta}{\partial \varphi} - \frac{V_\varphi}{R^2} \right] - 2 V_\theta \omega \cos \theta \end{aligned} \quad (2)$$

$$\begin{aligned}
& \frac{\partial V_\theta}{\partial t} + \frac{1}{R} \frac{\partial}{\partial \varphi} \left[ V_\varphi V_\theta - \frac{v}{R} \frac{\partial V_\theta}{\partial \varphi} + \overline{v'_\varphi v'_\theta} \right] + \frac{1}{Rr} \frac{\partial}{\partial \theta} \left[ R V_\theta V_\theta - \frac{vR}{r} \frac{\partial V_\theta}{\partial \theta} + R \overline{v'_\theta v'_\theta} \right] = \\
& - \frac{1}{\rho r} \frac{\partial P}{\partial \theta} + \frac{V_\varphi^2}{R} \cos \theta + \frac{\overline{v'_\varphi v'_\varphi}}{R} \cos \theta + v \left[ -\frac{2 \cos \theta}{R^2} \frac{\partial V_\varphi}{\partial \varphi} - \frac{V_\theta \cos^2 \theta}{R^2} - \frac{V_\theta}{r^2} \right] + \\
& + 2V_\varphi \omega \cos \theta + \omega^2 R \cos \theta
\end{aligned} \tag{3}$$

These equations, together with the turbulence kinetic energy  $\kappa$  and of the dissipation rate of the turbulence kinetic energy  $\varepsilon$ , presented below, are developed through the finite volumes method. The pressure-velocity coupling is made through the SOLA algorithm and the convective scheme QUICK is used. The development of the methodology used in the present work can be found in Pirani (1996).

The  $\kappa$ - $\varepsilon$  turbulence model equations, considering the toroidal regenerative turbomachine coordinates system are:

- Equation for the turbulence kinetic energy  $\kappa$

$$\begin{aligned}
& \frac{\partial \kappa}{\partial t} + \frac{1}{Rr} \frac{\partial}{\partial \varphi} \left( r \kappa V_\varphi - \frac{r}{R} \frac{v_t}{\sigma_\kappa} \frac{\partial \kappa}{\partial \varphi} \right) + \frac{1}{Rr} \frac{\partial}{\partial \theta} \left( r \kappa V_\theta - \frac{R}{r} \frac{v_t}{\sigma_\kappa} \frac{\partial \kappa}{\partial \theta} \right) = \\
& 2 v_t \left[ \left( \frac{1}{R} \frac{\partial V_\varphi}{\partial \varphi} + \frac{V_\theta \cos \theta}{R} \right)^2 + \left( \frac{1}{r} \frac{\partial V_\theta}{\partial \theta} \right)^2 + \frac{1}{2} \left( \frac{1}{r} \frac{\partial V_\varphi}{\partial \theta} - \frac{V_\varphi \cos \theta}{R} + \frac{1}{R} \frac{\partial V_\theta}{\partial \varphi} \right)^2 \right] - \varepsilon
\end{aligned} \tag{4}$$

- Equation for the dissipation rate of the turbulence kinetic energy  $\varepsilon$

$$\begin{aligned}
& \frac{\partial \varepsilon}{\partial t} + \frac{1}{Rr} \frac{\partial}{\partial \varphi} \left( r \varepsilon V_\varphi - \frac{r}{R} \frac{v_t}{\sigma_\varepsilon} \frac{\partial \varepsilon}{\partial \varphi} \right) + \frac{1}{Rr} \frac{\partial}{\partial \theta} \left( r \varepsilon V_\theta - \frac{R}{r} \frac{v_t}{\sigma_\varepsilon} \frac{\partial \varepsilon}{\partial \theta} \right) = \\
& 2 C_{\varepsilon 1} \frac{\varepsilon}{\kappa} v_t \left[ \left( \frac{1}{R} \frac{\partial V_\varphi}{\partial \varphi} + \frac{V_\theta \cos \theta}{R} \right)^2 + \left( \frac{1}{r} \frac{\partial V_\theta}{\partial \theta} \right)^2 + \frac{1}{2} \left( \frac{1}{r} \frac{\partial V_\varphi}{\partial \theta} - \frac{V_\varphi \cos \theta}{R} + \frac{1}{R} \frac{\partial V_\theta}{\partial \varphi} \right)^2 \right] - C_{\varepsilon 2} \frac{\varepsilon^2}{\kappa}
\end{aligned} \tag{5}$$

- Equation for the Boussinesq eddy-viscosity

$$-\overline{v'_r v'_r} = 2v_t \left[ \frac{\partial V_r}{\partial r} \right] - \frac{2}{3} \kappa \tag{6}$$

$$-\overline{v'_\varphi v'_\varphi} = 2v_t \left[ \frac{V_r \sin \theta}{R} + \frac{1}{R} \frac{\partial V_r}{\partial r} + \frac{V_\theta \cos \theta}{R} \right] - \frac{2}{3} \kappa \tag{7}$$

$$-\overline{v'_\theta v'_\theta} = 2v_t \left[ \frac{V_r}{r} + \frac{1}{r} \frac{\partial V_\theta}{\partial \theta} \right] - \frac{2}{3} \kappa \tag{8}$$

$$-\overline{v'_r v'_\varphi} = -\overline{v'_\varphi v'_r} = v_t \left[ \frac{\partial V_\varphi}{\partial r} + \frac{1}{R} \frac{\partial V_r}{\partial \varphi} - \frac{V_\varphi \sin \theta}{R} \right] \tag{9}$$

$$-\overline{v'_r v'_\theta} = -\overline{v'_\theta v'_r} = v_t \left[ \frac{\partial V_\theta}{\partial r} + \frac{1}{r} \frac{\partial V_r}{\partial \theta} - \frac{V_\theta}{r} \right] \tag{10}$$

$$-\overline{v'_\varphi v'_\theta} = -\overline{v'_\theta v'_\varphi} = v_t \left[ \frac{1}{R} \frac{\partial V_\theta}{\partial \varphi} + \frac{1}{r} \frac{\partial V_\varphi}{\partial \theta} - \frac{V_\varphi \cos \theta}{R} \right] \tag{11}$$

## 4. Initial and boundary conditions

### 4.1. Boundary conditions for the velocity components

Using a movable probe parallel to the straight board of the blades, with a distance of 5 mm from this, as shown in the Figure 6, Varella measured the values of the recirculation velocity  $C_m$  and tangential velocity  $C_u$  in different radial positions. The measured values in the corresponding positions of the mean effect streamline, are used as boundary conditions.

The Figure 7 presents the flow surface developed on a plan, as described in the item 2. As boundary condition in the inlet, a uniform velocity profile is used, whose value corresponds to the recirculation velocity, was obtained by Varella. In the outlet, due to the regenerative condition, the velocity profile is admitted identical to the inlet. Along the line a-b, in the area without blades, is imposed as boundary condition, the tangential velocity measured by Varella, due to the periodicity condition, the velocity profile along the line a'-b' is admitted identical to the a-b line.

In the blades the no-slip and impenetrability condition are admitted.

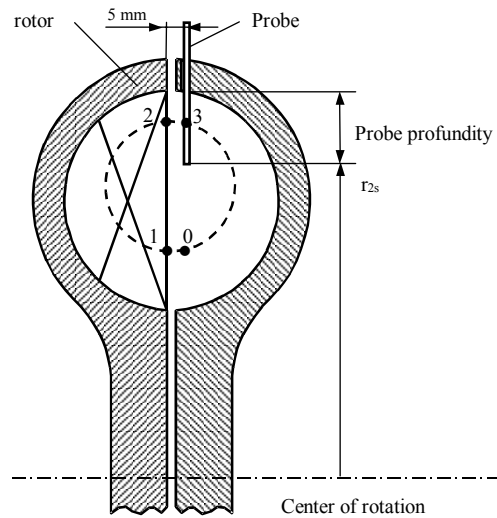


Figure 6. Probe position.

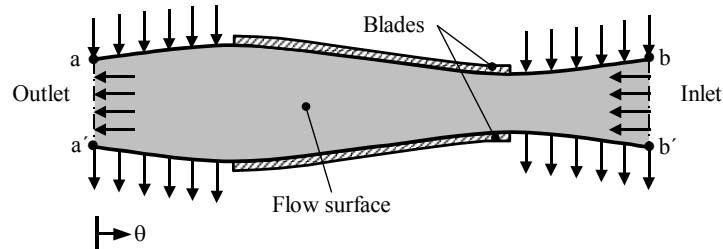


Figure 7. Flow surface developed on a plan.

### 4.2. Boundary conditions for turbulent quantities

#### • Inlet and outlet boundary conditions:

The turbulence kinetic energy  $\kappa$  and the dissipation rate of turbulence kinetic energy  $\varepsilon$  are admitted uniforms in the inlet, according to Pun and Spalding (1977) and Lin (1989):

$$\kappa = 0.005 U^2 \quad (12)$$

$$\varepsilon = C_\mu \frac{\kappa^{3/2}}{0.03 \zeta / 2} \quad (13)$$

where  $U$  is the inlet average velocity,  $\zeta$  is the width of the flow surface in the entrance and  $C_\mu$  is a constant with value 0.09.

Due to the regenerative condition, the boundary conditions in the outlet are identical to the one of inlet.

- Boundary conditions in the wall:

To avoid the use of an excessive number of control volumes in the regions close to the wall and the use of more complex turbulence models that take into account the abrupt variations that happen in the flow in those regions, wall functions are used.

## 5. Results

In this item, comparisons between the results obtained in the present work with those obtained experimentally by Varella (1981) and those obtained theoretically by Ramirez (1996) are made. The main characteristics of the studied toroidal regenerative turbomachine are: 24 blades, blade thickness of 6 mm, external radius of 130 mm, internal radius of 45 mm.

### 5.1. Slip factor

The slip factor is defined as:

$$\xi = \frac{C_{u3}}{U_2} \quad (14)$$

where  $U_2$  and  $C_{u3}$  are respectively the tangential velocity of the blade and the tangential velocity of the fluid in the points 2 and 3 shown in the Figure 6.

The table 1 presents values obtained by Varella (1981), for the slip factor  $\xi$ , in different depths of the probe and different flow rate coefficients  $\phi$ . The quantities  $r_1$ ,  $r_2$  and  $R_o$  represent, respectively, the internal, external and the center of circulation radius of mean effect streamline, according to Figure 2, and the quantity  $r_{2s}$  represents the radius of the measurement position of the probe, as shown in the Figure 6.

The flow rate coefficient in the toroidal regenerative turbomachine is defined as:

$$\phi = \frac{Q}{A_c u_m} = \frac{c_{u_c}}{\omega r_m} \quad (15)$$

where  $\omega$  is the angular velocity of the rotor,  $Q$  is the flow rate of the turbomachine,  $u_m = \omega r_m$  is the tangential velocity calculated in the average radius of the toro,  $r_m$  and  $A_c$  is the area of the free transverse section of the side channel, as shown in Figure 2.

Table 1: Results obtained by Varella (1981).

$\phi$	$r_1$ (mm)	$r_2$ (mm)	$R_o$ (mm)	$r = R_o - r_1$ (mm)	depths of the probe (mm)	$r_{2s}$ (mm)	$\xi$
0.00	70.90	117.00	93.95	23.10	5.00	125.00	0.51
					10.00	120.00	0.53
					15.00	115.00	0.50
0.21	71.50	115.30	93.40	21.90	5.00	125.00	0.53
					10.00	120.00	0.57
					15.00	115.00	0.58
0.60	72.20	112.80	92.50	20.30	5.00	125.00	0.60
					10.00	120.00	0.66
					15.00	115.00	0.68
0.77	72.30	112.00	92.15	19.90	5.00	125.00	0.61
					10.00	120.00	0.62
					15.00	115.00	0.63
0.92	72.30	112.00	92.15	19.90	5.00	125.00	0.60
					10.00	120.00	0.72
					15.00	115.00	0.77

Considering the depth of the probe 5 mm, that corresponds on a radius,  $r_2$ , of 125 mm, the data for the slip factor obtained through computational program, the experimental data from Varella (1981), and the theoretical from Ramirez (1996) are presented in the Figure 8. It is observed that the results obtained by the present work are closer to the experimental results of Varella in relation to the theoretical results obtained by Ramirez, that neglect the effect of the viscosity, overestimating the values for the slip factor.

The same behavior is observed in the Figures 9a and 9b on which the depths of the probe are 10 and 15 mm, respectively. The proposed viscous flow model presents closer results to the experimental of Varella in relation to the ideal model of Ramirez.

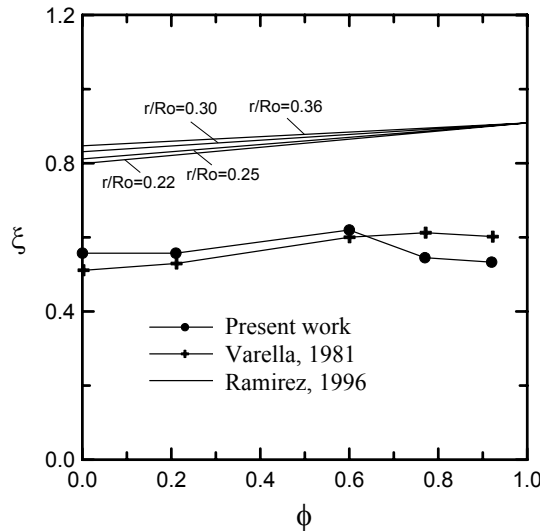


Figure 8. Theoretical and experimental Slip Factor to depth of the probe 10 mm.

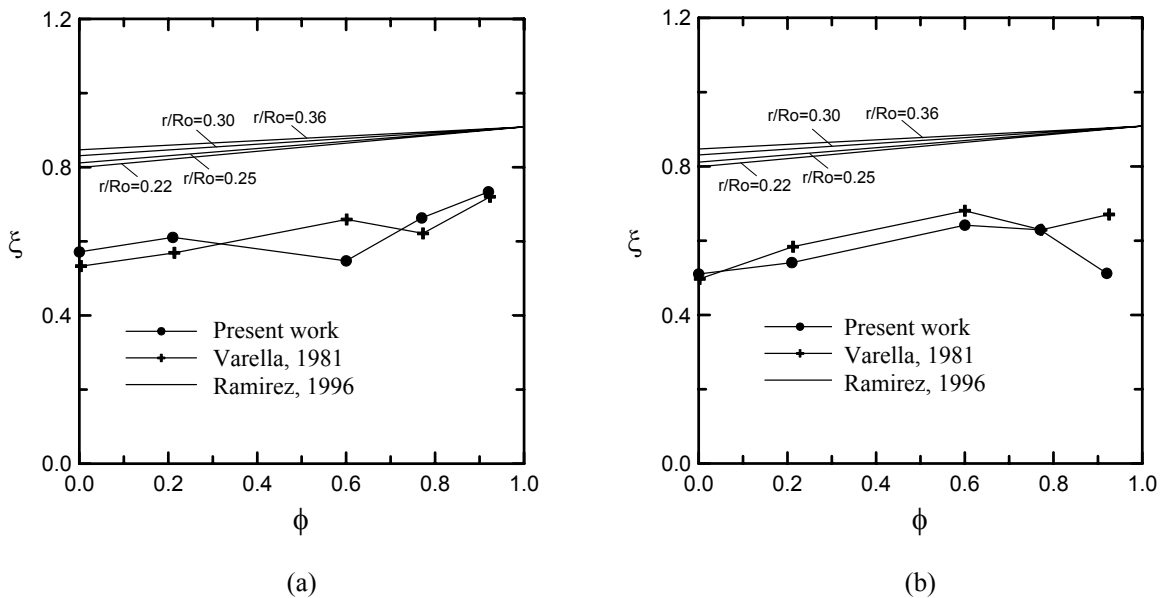


Figure 9. Theoretical and experimental Slip Factor to depth of the probe: (a) 10 mm; (b) 15 mm.

The Figure 10 presents the behavior of the slip factor in relation to the refinement of the mesh for a flow rate coefficient  $\phi$  equal to zero and the depth of the probe 10 mm. It is observed that for a number of elements bigger than 14000, that corresponds for instance to a mesh 60x240, the slip factor tends to a constant value. To maintain the time of processing around 12 hours, using a computer Pentium IV with 256 MB of RAM memory and compiler FORTRAN Power Station IV, a uniform mesh 60x240 was adopted in the final results.

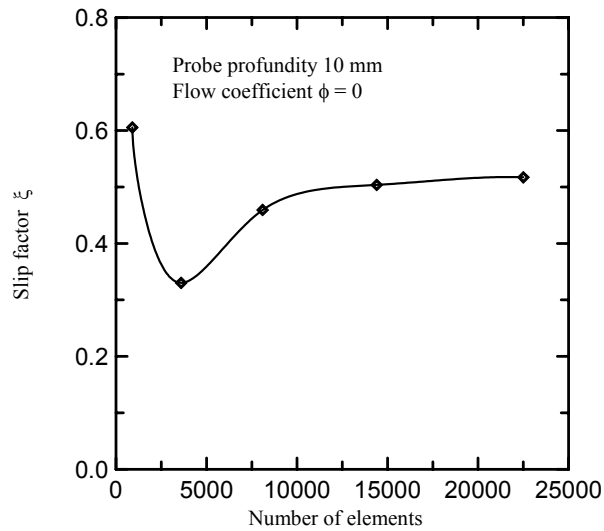


Figure 10. Behavior of the slip factor in function of the number of elements for  $\phi = 0,00$  , depth of the probe 10mm.

## 5.2. Head coefficient

In the Figures 11a and 11b, comparisons are made between the head coefficients obtained in the present work, with the experimental of Varella (1981), for flow coefficients of 0.00 and 0.60, respectively. The pressure coefficient used is defined as:

$$\psi_R = \frac{2 \Delta P}{\rho u_m^2} \quad (16)$$

where  $\Delta P$  is the difference pressure obtained through the computer program (blade to blade),  $\rho$  is the density equal to  $1.165 \text{ kg/m}^3$  and  $u_m$  is the tangential velocity in the radius  $r_m$  of the geometric center of the toro ( $u_m = \omega r_m$ ).

The head coefficient was determined considering the mean effect streamline, represented by the radius  $r_1$  and  $r_2$  presented in Table 1. The difference pressure value  $\Delta P$  and, consequently, the value of  $\psi_R$ , obtained through the computer program, corresponds to the region between two consecutive blades. To the rotor in question, that is composed by 24 blades, the angle between two consecutive blades  $\phi$  is 15 degrees. On the results, as the comparison range is of 150 degrees in the least disturbed region, the value of the head coefficient was multiplied by 10.

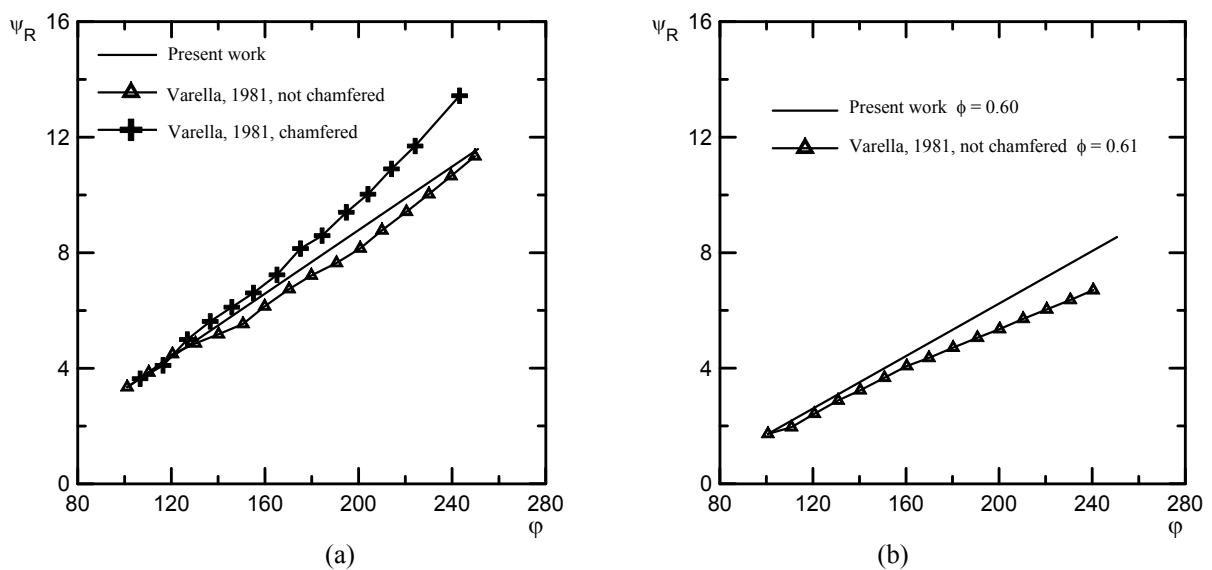


Figure 11. Theoretical and experimental head coefficient in function of the angle  $\phi$  of the toro. (a)  $\phi = 0.00$  ; (b)  $\phi = 0.60$  from the present work and  $\phi = 0.61$  from Varella (1981).

The head coefficient graph from the inlet to outlet of the machine, related to the flow rate coefficient is presented in the Figure 12. The results obtained with the computer program developed in the present work are compared with the experimental of Varella (1981), considering two conditions: in the first condition, Varella obtained the results using a rotor with not chamfered blades and, in the second condition, Varella used a rotor with 30 degrees chamfered blades.

The difference pressure value obtained with the computer program and used in the calculus of the head coefficient, defined by the Equation 16, was, in this case, multiplied by 20, because the angle between the entrance and the exit of the machine is of 300 degrees and, to the considered rotor, the angle between two consecutive blades is of 15 degrees.

It is observed on this graph, to higher flow rate coefficients, the values of the head coefficient, obtained in the present work, are higher than that obtained experimentally. This fact can be justified, considered that, higher flow rate coefficients means higher losses happen in the inlet and outlet openings of the machine, due to higher average velocity of the flow, reducing the head coefficient value. The same doesn't happen with the results obtained in the present work, that doesn't consider those losses.

Another justification for the behavior of the theoretical curve, shown in the Figure 12, can be the turbulence model used. The turbulence model  $\kappa$ - $\epsilon$  was developed for high Reynolds numbers, when the machine works with low flow rate coefficients, the fluid circulates a larger number of times to the channels, with a larger recirculation velocity, and therefore, with larger local Reynolds number. The opposite is observed to high flow rate coefficients.

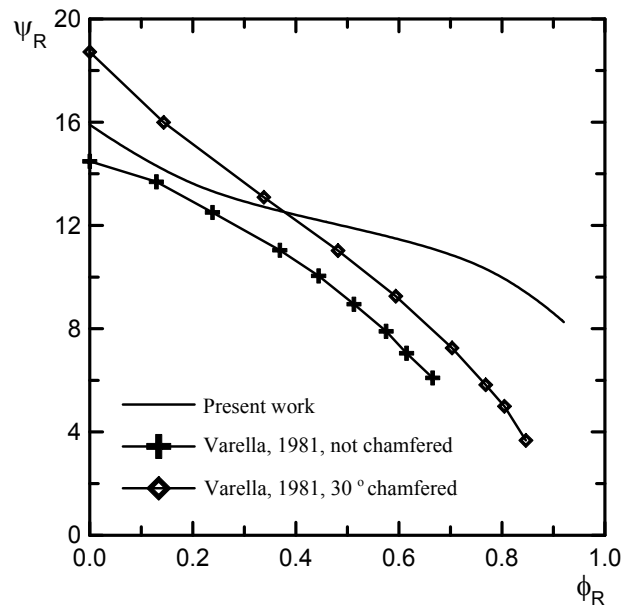


Figure 12. head coefficients related to the flow rate coefficients.

### 5.3. Vorticity

In the Table 2, values for the non-dimensional average vorticity are presented in several flow conditions. In agreement with the Stokes theorem, the circulation along the boundary that defines the region of the flow is equal to the integral of the vorticity on the corresponding region. In the specific case of the toroidal regenerative turbomachines, due to the regenerative and periodicity conditions, imposed in the border, the circulation and, consequently, the integral of the vorticity are null. Thereby, an important parameter for the qualitative analysis of the results, obtained through the computer program, is the non-dimensional average vorticity, defined according to the Equation 17, that should satisfy the Stokes theorem. The largest value found for the non-dimensional average vorticity was of 0.0001442.

$$\Omega_{\text{adim}} = \frac{\sum_i \Omega_i \Delta A_i}{\omega A_{\text{tot}}} \quad (17)$$

where  $\Delta A_i$  is the corresponding area of the flow surface whose the value of the vorticidade is  $\Omega_i$ ,  $A_{\text{tot}}$  is the total area of the flow surface and  $\omega$  is the angular velocity of the rotor in rad/s.

Table 4.2: Non-dimensional average vorticity for different flow rate coefficients and depths of the probe.

Flow rate coefficients	Non-dimensional average vorticity		
	e = 5mm	e = 10mm	e = 15mm
0	$-7.19 \times 10^{-5}$	$-9.07 \times 10^{-5}$	$-7.44 \times 10^{-5}$
0.21	$1.75 \times 10^{-5}$	$5.82 \times 10^{-5}$	$-10.88 \times 10^{-5}$
0.60	$-1.48 \times 10^{-5}$	$14.42 \times 10^{-5}$	$-1.82 \times 10^{-5}$
0.77	$-7.70 \times 10^{-5}$	$2.02 \times 10^{-5}$	$3.26 \times 10^{-5}$
0.92	$-6.40 \times 10^{-5}$	$2.03 \times 10^{-5}$	$3.07 \times 10^{-5}$

## 6. Conclusion

Related to the results obtained for the toroidal regenerative turbomachine, in spite of the limitations of the proposed modelling, it was possible to get some characteristics of that machine, such as slip factor, head coefficient besides the qualitative verification of the results through the prove of the Stokes theorem.

The recirculation velocity, that at first sign was supposed that could be resulting of the calculations, had to be imposed as boundary condition, it is believed that, this velocity will only result of the calculations for a three-dimensional modelling of the flow.

After the implementation of the toroidal regenerative turbomachine coordinates, in the computer program, together with the non-inertial effects, represented by the Coriolis and centrifuge acceleration, the convergence time increased considerably, in spite of that, the SOLA method has shown quite stable. The convergence of the SOLA method can be accelerated through the modifications proposed by Tomiyama et al (1994).

Most of the time used in the development of the present work was aimed to the computer program elaboration and execution. Great difficulties were found, to that, it is advisable to structure the program through subroutines, to a larger control of the changes and possible errors. Plenty caution should be taken in the implementation of the wall laws.

The computer program presents limitations, on depending of experimental data in the application of the boundary conditions, however, defined those conditions, the program allows the study of the toroidal regenerative turbomachines with different relationships of radius  $r/R_0$  and different number of blades.

## 7. References

- Lin Chau Jen , 1989, "Modelo Matemático para Escoamento Turbulento Confinado, Visando a Configuração de Queimadores para Gases de Petróleo e outros Gases Industriais", Master Thesis of Polytechnic School from São Paulo University.
- Pirani, M. J., 1996, "Simulação de Escoamentos Turbulentos Usando o Método dos Volumes Finitos", Master Thesis of Federal School of Engineering of Itajubá, Itajubá, Minas Gerais.
- Pun , W. M. & Spalding, D. B., 1977, "A General Computer Program for Two - Dimensional Elliptic Flows", Imperial College of Science and Technology.
- Ramirez, R. G. C., 1996, "Análise do Escoamento em Grades Regenerativas", Master Thesis of Federal School of Engineering of Itajubá.
- Tomiyama, A., Hirano, M., 1994, "An Improvement of the Computational Efficiency of the SOLA Method", JSME International Journal, Series B, Vol. 37 No 4, pp. 821-826.
- Varella, S., 1981, "A Theoretical and Experimental Analysis of Regenerative Blowers", Ph.D. Thesis, Southampton University.